

A Facile One-Pot Synthesis of Hydroxyl-Functionalized Gold Polyhedrons by a Surface Regulating Copolymer

Choong Il Yoo,[†] Daeha Seo,[†] Bong Hyun Chung,[‡] Im Sik Chung,^{*,‡} and Hyunjoon Song^{*,†}

Department of Chemistry and School of Molecular Science (BK21), Korea Advanced Institute of Science and Technology, Daejeon 305-701, Korea, and BioNanotechnology Research Center, Korea Research Institute of Bioscience and Biotechnology (KRIBB), Daejeon 305-333, Korea

Received October 21, 2008. Revised Manuscript Received January 8, 2009

We report a simple, one-pot process for hydroxyl-functionalized gold nanocrystals with precise morphology control by a surface regulating copolymer. The copolymer, poly(vinyl pyrrolidone-*ran*-vinyl acetate) (PVP-PVAc), has two distinct moieties including pyrrolidone for nanoparticle formation and acetate for additional functionalization. The particle sizes are readily controlled in the range of 35–80 nm by changing the solvent volume, and the shapes are tuned from octahedral to cuboctahedral and cubic by the addition of AgNO₃. Concomitantly, hydrolysis of the acetate groups during the reaction generates multiple hydroxyl groups on the particle surface, which can readily conjugate with versatile functionalities through esterification. This copolymer-based process achieves the synthesis, morphology control, and functionalization of gold nanocrystals via a one-step reaction, as this is superior to the other multistep synthetic procedures.

Introduction

Gold nanocrystals are the most stable metallic nanostructures and have been intensively studied in materials science.¹ The behavior of individual particles as well as their size- and shape-related electronic, optical, and catalytic properties make gold nanocrystals a fascinating material for a wide range of applications including molecular recognition,² sensors,³ drug delivery,⁴ biomedical imaging,⁵ and photothermal therapy.⁶ For general applications, gold nanocrystals

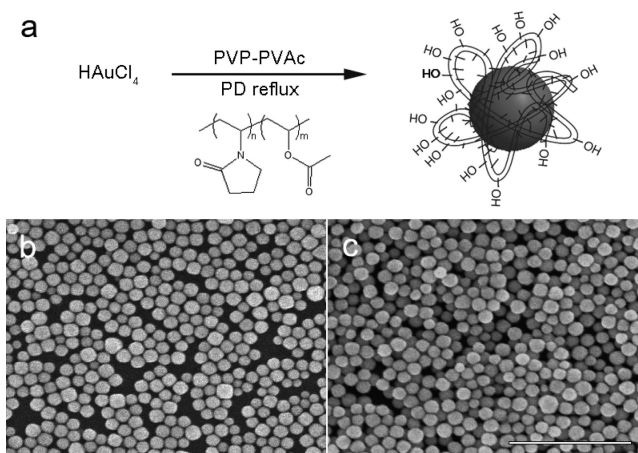


Figure 1. (a) One-pot synthesis of hydroxyl-functionalized gold nanocrystals using PVP-PVAc. SEM images of the gold nanocrystals synthesized using (b) PVP-PVAc and (c) pure PVP. The bar represents 500 nm.

must be stabilized by ligands or surfactants in order to prevent their coagulation.⁷

For biological applications, gold nanocrystals must be stable and dispersed well in aqueous media, and readily conjugated with biomolecules through reactive functional groups on their surface. Generally, thiols containing carboxylate or poly(ethylene oxide) units are incorporated in water-soluble gold nanocrystals by ligand exchange.⁸ Other ligands of choice are polymers with polar groups such as

* Corresponding author. E-mail: cis123@kribb.re.kr (I.S.C.); hsong@kaist.ac.kr (H.S.).

[†] Korea Advanced Institute of Science and Technology.

[‡] Korea Research Institute of Bioscience and Biotechnology.

- (1) (a) Danial, M.-C.; Astruc, D. *Chem. Rev.* **2004**, *104*, 293–346. (b) Eustics, S.; El-Sayed, M. A. *Chem. Soc. Rev.* **2006**, *35*, 209–217.
- (2) (a) Park, S. J.; Taton, T. A.; Mirkin, C. A. *Science* **2002**, *295*, 1503–1506. (b) Park, S. J.; Lazarides, A. A.; Mirkin, C. A.; Letsinger, R. L. *Angew. Chem., Int. Ed.* **2001**, *40*, 2909–2912.
- (3) (a) Haes, A. J.; Haynes, C. L.; McFarland, A. D.; Schatz, G. C.; Van Duyne, R. P.; Zou, S. *MRS Bull.* **2005**, *30*, 368–375. (b) Zhu, M.; Wang, L.; Exarhos, G. J.; Li, A. D. Q. *J. Am. Chem. Soc.* **2004**, *126*, 2656–2657. (c) Rex, M.; Hernandez, F. E.; Campiglia, A. D. *Anal. Chem.* **2006**, *78*, 445–451.
- (4) (a) West, J. L.; Halas, N. J. *Curr. Opin. Biotechnol.* **2000**, *11*, 215–217. (b) Gelperina, S.; Kisich, K.; Iseman, M. D.; Heifets, L. *Am. J. Respir. Crit. Care Med.* **2005**, *172*, 1487–1490.
- (5) (a) Qian, X.; Peng, X.-H.; Ansari, D. O.; YinGoen, Q.; Chen, G. Z.; Shin, D. M.; Yang, L.; Young, A. N.; Wang, M. D.; Nie, S. *Nat. Biotechnol.* **2008**, *26*, 83–90. (b) Wang, H.; Huff, T. B.; Zweifel, D. A.; He, W.; Low, P. S.; Wei, A.; Cheng, J. X. *Proc. Natl. Acad. Sci. U.S.A.* **2005**, *102*, 15752–15756. (c) Eghtedari, M.; Oraevsky, A.; Copland, J. A.; Kotov, N. A.; Conjusteau, A.; Motamedi, M. *Nano Lett.* **2007**, *7*, 1914–1918.
- (6) (a) Huang, X.; El-Sayed, I. H.; Qian, W.; El-Sayed, M. A. *J. Am. Chem. Soc.* **2006**, *128*, 2115–2120. (b) Hirsch, L. R.; Stafford, R. J.; Bankson, J. A.; Sershen, S. R.; Rivera, B.; Price, R. E.; Hazle, J. D.; Halas, N. J.; West, J. L. *Proc. Natl. Acad. Sci. U.S.A.* **2003**, *100*, 13549–13554.
- (7) (a) Templeton, A. C.; Wuelfing, W. P.; Murray, R. W. *Acc. Chem. Res.* **2000**, *33*, 27–36. (b) Brust, M.; Walker, M.; Bethell, D.; Schiffrin, D. J.; Whyman, R. J. *Chem. Soc., Chem. Commun.* **1994**, 801–802.

- (8) (a) Yoo, H.; Momozawa, O.; Hamatani, T.; Kimura, K. *Chem. Mater.* **2001**, *13*, 4692–4697. (b) Chen, S.; Kimura, K. *Langmuir* **1999**, *15*, 1075–1082. (c) Wuelfing, W. P.; Gross, S. M.; Miles, D. T.; Murray, R. W. *J. Am. Chem. Soc.* **1998**, *120*, 12696–12697.
- (9) (a) Bonet, F.; Delmas, V.; Grugeon, S.; Herrera Urbina, R.; Silvert, P.-Y.; Tekaia-Elhsissen, K. *Nanostruct. Mater.* **1999**, *11*, 1277–1284. (b) Silvert, P.-Y.; Tekaia-Elhsissen, K. *Solid State Ionics* **1995**, *82*, 53–60.

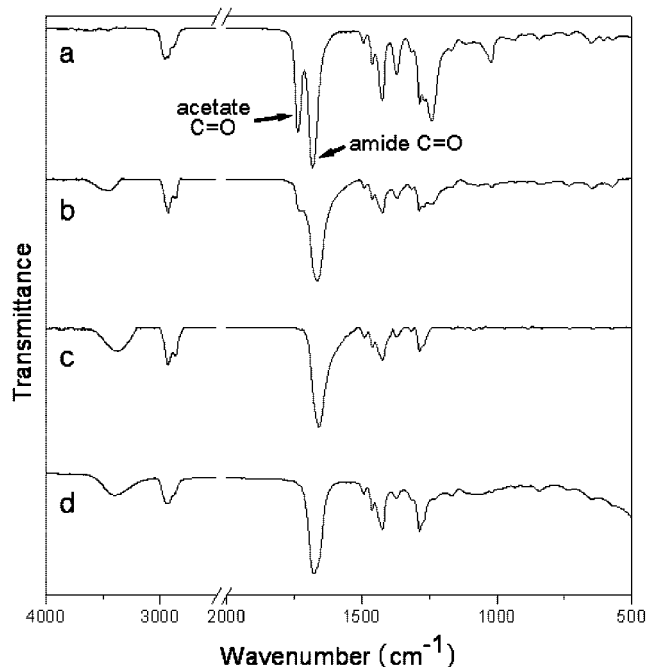


Figure 2. IR spectra of (a) free PVP-PVAc, (b) gold nanocrystals synthesized with PVP-PVAc after 1 h reflux, (c) gold nanocrystals under the same condition after 5 h reflux, and (d) free PVP-PVA converted from PVP-PVAc by saponification.

poly(vinyl pyrrolidone) (PVP)⁹ and poly(acrylic acid).¹⁰ PVP, in particular, shows good biocompatibility with low toxicity for living tissues, and has been used as a ‘magic’ polymer for controlling both the size and shape of metallic nanocrystals at the same time.¹¹ Recently, we have reported the shape engineering of polyhedral gold nanocrystals in the presence of PVP.¹² For further functionalization, however, PVP is hardly exchangeable with other ligands because of its multiple coordination on the metal surface.

In this study, we report a simple, one-pot process for hydroxyl-functionalized gold nanocrystals with precise morphology control by a surface regulating copolymer. The copolymer has two distinct moieties, including pyrrolidone for nanoparticle formation and acetate for functionalization. We have successfully synthesized various gold polyhedrons containing multiple hydroxyl groups in the presence of poly(vinyl pyrrolidone-*ran*-vinyl acetate) (PVP-PVAc). This copolymer-based process achieves the synthesis, morphology control, and functionalization of gold nanocrystals via a one-pot reaction.

Experimental Section

Chemicals. HAuCl₄ (99.9+%, Aldrich), AgNO₃ (99+%, Aldrich), 1,5-pentanediol (PD, 96%, Aldrich), PVP-PVAc (*M_w* =

50 000, VP:VAc = 1.3 molar ratio, Aldrich), ethanol (99.9%, J. T. Baker), methanol (99.8%, Junsei), chloroform (99.0%, Junsei), HCl (35.0%, Junsei), *N,N*-dimethylacetamide (DMAc, 99%, Junsei), triethylamine (99.5%, Aldrich), acetyl chloride (98%, Aldrich), lauroyl chloride (98%, Aldrich), and pentadecafluorooctanoyl chloride (97%, Aldrich) were used as received.

Synthesis of Gold Nanocrystals with PVP-PVAc. A solution of AgNO₃ (0.15 mL, 0.020 M) in PD was added to boiling PD (21 mL). PVP-PVAc (6.0 mL, 0.270 g) and HAuCl₄ (3.0 mL, 0.050 M) solutions in PD were added periodically every 30 s over 7.5 min. The resulting mixture was heated at reflux for 5 h to ensure complete hydrolysis of PVP-PVAc. The product was washed by several precipitation–dispersion cycles with ethanol. The copolymer-capped gold nanocrystals were finally dispersed in ethanol (30 mL). For gold nanocrystals capped with PVP, the synthesis followed the same procedure except the use of PVP instead of PVP-PVAc.

Size Control of Gold Nanocrystals. The procedure is identical to that of the gold nanocrystals with PVP-PVAc except the solvent volume used in the reactions. For the gold spheres with 35, 50, and 80 nm diameters, 31, 21, and 11 mL of boiling PD were used, respectively.

Shape Control of Gold Nanocrystals. The same procedure as for the gold spheres was followed except the AgNO₃ concentrations. The AgNO₃ concentrations added to the reaction mixture were 5.0 mM for cubes, 3.3 mM for cuboctahedrons, and 1.7 mM for octahedrons, respectively.

Saponification of PVP-PVAc. PVP-PVAc (10 g) was dissolved in methanol (250 mL) and added sodium hydroxide (1.6 g, 40 mmol). The reaction mixture was refluxed for 24 h to ensure complete hydrolysis of PVP-PVAc. After the reaction, the mixture was neutralized by HCl addition. Dialysis of the product in water yielded pure PVP-PVAc.

Esterification of Hydroxyl-Functionalized Gold Nanocrystals. The hydroxyl-functionalized gold nanocrystals were dispersed in DMAc (5.0 mL). Triethylamine (0.56 mL, 4.0 mmol) was slowly added, and acyl chloride (4.1 mmol) was then added dropwise to the reaction mixture and the total volume of the mixture was fixed to 10 mL by adding DMAc. Acetyl chloride (0.30 mL), lauroyl chloride (0.99 mL), and pentadecafluorooctanoyl chloride (1.05 mL) were used for the reactions. The resulting mixture was stirred for 24 h at room temperature. The product was thoroughly washed with chloroform and ethanol by several precipitation–dispersion cycles.

Characterization. Scanning electron microscopy (SEM) images were obtained using a Philips XL30S FEG operated at 10 kV. Fourier transform-infrared (FT-IR) spectroscopy data were collected on a BRUKER EQUINOX55 spectrometer. The samples were prepared by a few drops of the colloidal solutions on a silicon wafer (P-100) followed by drying in air. The UV–vis absorption data were recorded on a Jasco V530 UV–vis spectrophotometer using colloidal ethanol suspensions. Thermodynamic analysis (TGA) was performed on a TA 2200 Thermal Analyzer system. TGA measurements were carried out at a heating rate of 10 °C/min in N₂. Dynamic light scattering (DLS) measurements were performed using a 90 Plus Particle Size Analyzer (Brookhaven Instruments Corporation) with the sample dispersions in ethanol at room temperature.

Results and Discussion

Synthesis and Characterization of Hydroxyl-Functionalized Gold Nanocrystals with PVP-PVAc. The gold nanocrystals using PVP-PVAc were synthesized through a modified polyol process. Briefly, a total of 6.0 mL of PVP-PVAc and 3.0 mL of 0.050 M HAuCl₄ solutions in 1,5-pentanediol

- (10) (a) Ahmadi, T. S.; Wang, Z. L.; Green, T. C.; Henglein, A.; El-Sayed, M. A. *Science* **1996**, 272, 1924–1925. (b) Petroski, J. M.; Wang, Z. L.; Green, T. C.; El-Sayed, M. A. *J. Phys. Chem. B* **1998**, 102, 3316–3320.
- (11) (a) Wiley, B.; Sun, Y.; Xia, Y. *Acc. Chem. Res.* **2007**, 40, 1067–1076. (b) Wiley, B.; Sun, Y.; Chen, J.; Cang, H.; Li, Z.-Y.; Li, X.; Xia, Y. *MRS Bull.* **2005**, 30, 356–361. (c) Sun, Y.; Xia, Y. *Science* **2002**, 298, 2176–2179.
- (12) (a) Seo, D.; Yoo, C. I.; Park, J. C.; Park, S. M.; Ryu, S.; Song, H. *Angew. Chem., Int. Ed.* **2008**, 47, 763–767. (b) Seo, D.; Yoo, C. I.; Chung, I. S.; Park, S. M.; Ryu, S.; Song, H. *J. Phys. Chem. C* **2008**, 112, 2469–2475. (c) Seo, D.; Park, J. C.; Song, H. *J. Am. Chem. Soc.* **2006**, 128, 14863–14870.

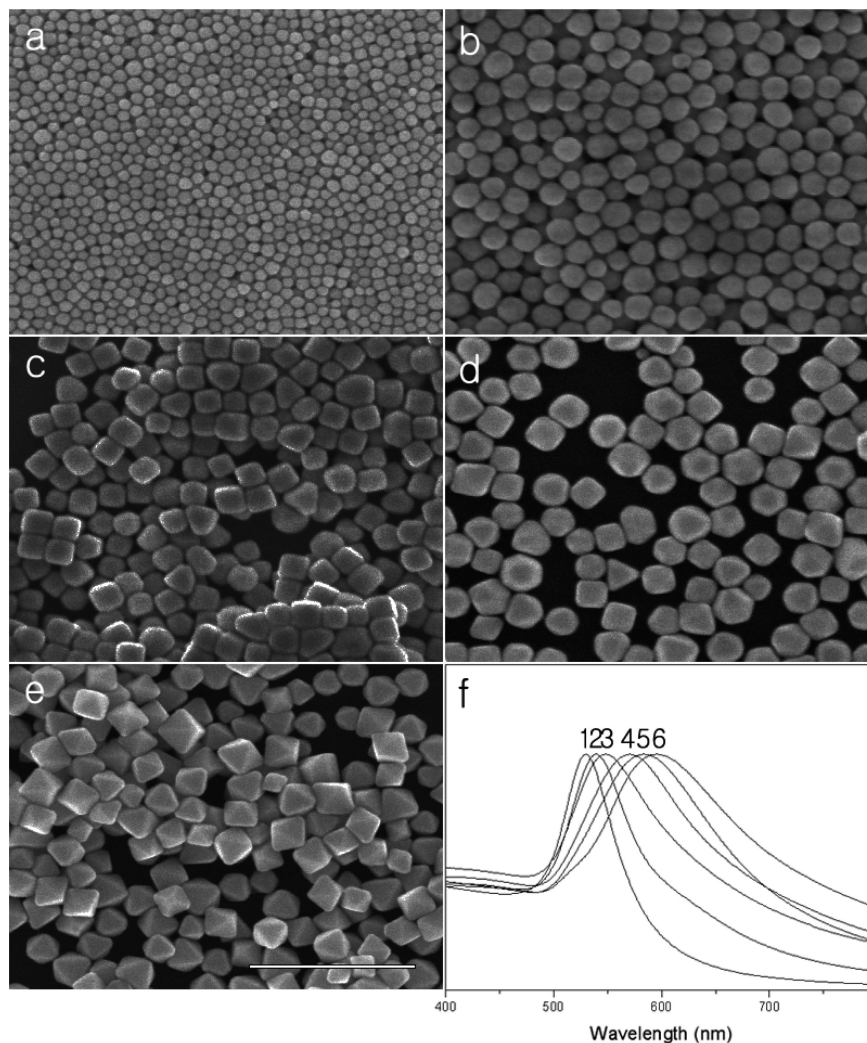


Figure 3. Size- and shape-controlled gold nanocrystals using PVP-PVAc. SEM images of (a) small gold nanocrystals with the average diameter of 35 ± 4 nm, (b) large gold nanocrystals with a diameter of 80 ± 10 nm, (c) gold nanocubes with an edge length of 70 ± 6 nm, (d) gold nanocuboctahedrons with an edge length of 85 ± 9 nm, and (e) gold nanooctahedrons with an edge length of 90 ± 10 nm. The bar represents 500 nm. (f) UV extinction spectra of (1–3) spherical particles with 35, 50, and 80 nm diameters, and (4–6) gold cubes, cuboctahedrons, and octahedrons, respectively.

(PD) were periodically added every 30 s over 7.5 min to 21 mL of boiling PD containing $3.0 \mu\text{mol}$ of AgNO_3 (1/50 equiv. with respect to the gold precursor). The reaction mixture was refluxed for 5 h to ensure complete hydrolysis of the acetate group in PVP-PVAc. After repetitive purification, copolymer-capped gold nanocrystals were obtained in a high yield. The resulting particles are very stable both at room temperature and under ethanol reflux for more than 5 h and maintain a good dispersion in acidic or basic conditions. Figure 1b shows that the particles are nearly spherical and monodisperse with an average diameter of 50 ± 5 nm. Gold nanocrystals using PVP were also synthesized via the same process, and their morphological features are identical to those of the particles using PVP-PVAc (Figure 1c), implying that the acetate units do not influence the particle formation.

The functionality of the polymers was characterized by IR spectroscopy. Pure PVP-PVAc presents two unique peaks assignable to the $\text{C}=\text{O}$ stretch. As shown in Figure 2a, the peak at 1735 cm^{-1} is from the carbonyl stretch of the acetate group, and the large peak at 1682 cm^{-1} is due to the amide

group of the vinyl pyrrolidone unit. The acetate $\text{C}=\text{O}$ stretch decreases slowly to become a shoulder after 1 h reflux of the reaction mixture (Figure 2b), and eventually disappears as the reaction time increases up to 5 h (Figure 2c). As well as diminishing the acetate stretching peak, a broad peak assignable to the hydroxyl group emerges at around 3400 cm^{-1} . The amide $\text{C}=\text{O}$ peak of the vinyl pyrrolidone unit gradually shifts to a lower energy level (1660 cm^{-1}) by 22 cm^{-1} because of strong coordination onto the gold surface. Similar redshifts of the IR stretching have been reported in silver and other noble metal powders.¹³ In order to confirm complete hydrolysis, the free PVP-PVAc polymer was treated by saponification without the gold precursor. The IR spectrum of the polymer (Figure 2d) contains hydroxyl and carbonyl stretching modes without any peaks from the acetate group, indicating the formation of PVP-PVA (poly(vinyl pyrrolidone-*ran*-vinyl alcohol)). The polymer IR spectrum also exactly matches the spectrum of the hydroxyl-function-

(13) (a) Bonet, F.; Tekaiia-Elhsissen, K.; Sarathy, K. V. *Bull. Mater. Sci.* **2000**, 23, 165–168. (b) Zhang, Z.; Zhao, B.; Hu, L. *J. Solid State Chem.* **1996**, 121, 105–110.

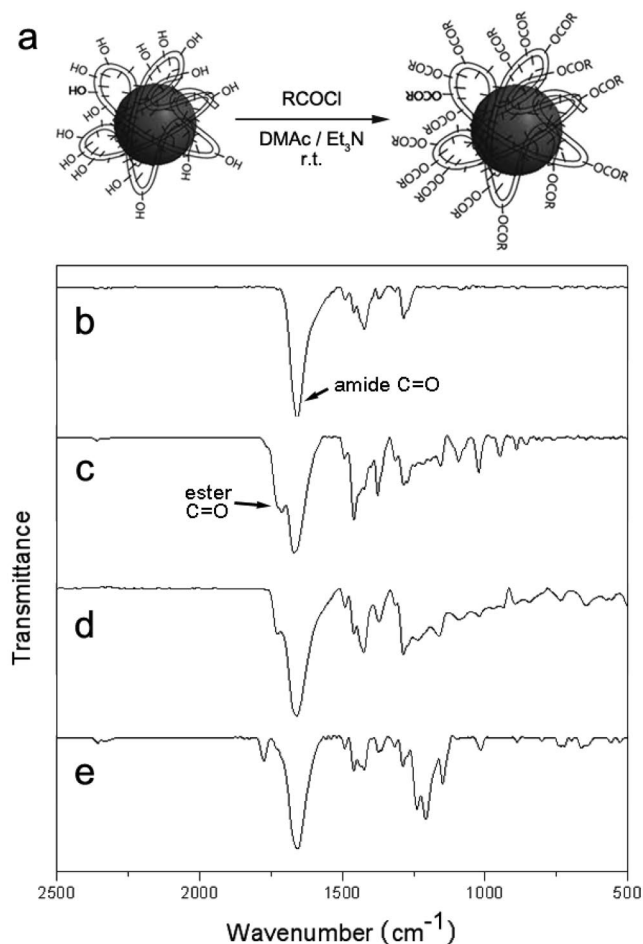


Figure 4. (a) Functionalization of gold nanocrystals through esterification. IR spectra of (b) hydroxyl-functionalized gold nanocrystals before esterification, and the gold nanocrystals after the reactions with (c) acetyl chloride, (d) lauroyl chloride, and (e) pentadecafluorooctanoyl chloride.

alized gold nanocrystals in Figure 2c. These IR spectral changes reveal that the acetate group of the PVP-PVAc was hydrolyzed concomitantly during the gold precursor reduction. This result is unexpected, but is easily understandable because our reaction condition is highly acidic owing to the gold precursor and the oxidation products of PD during the reaction. Such an acid-catalyzed hydrolysis is a well-known reaction in organic synthesis.¹⁴ The functionalization of gold nanocrystals is usually through a ligand place exchange, which requires excess thiols and a long reaction time for effective ligand substitutions.¹⁵ By contrast, our process uses a simple one-pot reaction to reduce a difficult purification procedure.

Morphology Control of Hydroxyl-Functionalized Gold Nanocrystals. The size of the spherical gold nanocrystals was controlled by changing the solvent volume. For example, particles with average diameters of 35 ± 4 and 80 ± 10 nm were obtained by using 31 and 11 mL of PD,

respectively (images a and b in Figure 3). This effect is attributed to the fact that higher precursor concentrations increase the collision frequency of either gold atoms or tiny gold nanocrystals with each other in solution to form larger particles through the Ostwald ripening process.¹⁶ The number of hydroxyl groups for each nanoparticle was quantitatively analyzed by thermogravimetric analysis (TGA). The polymer weight percent was directly derived from the total weight loss of gold nanocrystals at high temperature > 600 °C. As a result, the particles with 35, 50, and 80 nm diameters involve 1.3, 1.1, and 0.85 wt% of the polymers, respectively, because smaller particles have a higher surface area/volume ratio. In the 50 nm gold nanocrystals, the number of hydroxyl groups attached to the gold surface is estimated to be 45 000 per particle if all acetate groups were hydrolyzed completely. This value is comparable to that of the closed-packed monolayers of thiol ligands on the gold surface. According to our calculation, 20 wt % 6-mercapto-1-hexanol is able to cover the surfaces of all of the 2 nm gold nanoclusters, but only 1.2 wt % is required for the 50 nm nanocrystals.¹⁷ Considering that closed-packed monolayers of the ligands on the nanocrystals are hardly formed by a simple procedure, our copolymer-capped gold nanocrystals are superior to the thiol-functionalized gold nanocrystals in terms of multiple surface functionalities.

In the presence of PVP, we have reported that changing the dosage of AgNO_3 in the reaction mixture could control the gold nanoparticle shapes from octahedral to cubic and spherical.¹² Similar strategy was applied for PVP-PVAc, yielding various hydroxyl-functionalized gold polyhedrons. By the addition of 1/200, 1/400, and 1/600 equiv. of AgNO_3 with respect to the gold precursor concentration, the final gold nanocrystals were obtained as cubic, cuboctahedral, and octahedral, respectively (Figure 3c–e). This control over shape results from the preferential underpotential deposition of silver to Au(100) facets.¹² It is interesting to note that the UV–vis extinction peaks of the gold nanocrystals with different sizes and shapes exhibit redshifts in sequence with that of the small gold spheres (Figure 4f). The maximum extinction wavelengths (λ_{max}) are 530, 540, and 548 nm for the spheres with the diameters of 35, 50, and 80 nm, respectively. Such size-dependent extinction shifts in the spherical particles were analyzed by exact solutions of the Mie theory.¹⁸ The λ_{max} for cubes, cuboctahedrons, and octahedrons are 570, 583, and 596 nm, respectively. The shape-dependent optical properties are not as simple as the size dependency, but it is possible to analyze them by numerical calculations such as discrete dipole approximation and finite different time domain methods.¹⁹ In our experiments, each polyhedral gold nanocrystal exhibits a broad peak containing dipoles and quadrupoles together, and shows a unique maximum shift with respect to those of the spherical particles. In summary, controlling the size and shape of gold nanocrystals allows for tuning of the extinction maxima in the range of 530–600 nm, which is very important for

(14) Bender, M. L. *Chem. Rev.* **1960**, *60*, 53–113.

(15) (a) Hostetler, M. J.; Templeton, A. C.; Murray, R. W. *Langmuir* **1999**, *15*, 3782–3789. (b) Ingram, R. S.; Hostetler, M. J.; Murray, R. W. *J. Am. Chem. Soc.* **1997**, *119*, 9175–9178. (c) Hostetler, M. J.; Green, S. J.; Stokes, J. J.; Murray, R. W. *J. Am. Chem. Soc.* **1996**, *118*, 4212–4213.

(16) Hoang, T. K. N.; Deriemaeker, L.; La, V. B.; Finsy, R. *Langmuir* **2004**, *20*, 8966–8969.

(17) Tan, H.; Zhan, T.; Fan, W. Y. *J. Phys. Chem. B* **2006**, *110*, 21690–21693.

(18) Kelly, K. L.; Coronado, E.; Zhao, L. L.; Schatz, G. C. *J. Phys. Chem. B* **2003**, *107*, 668–677.

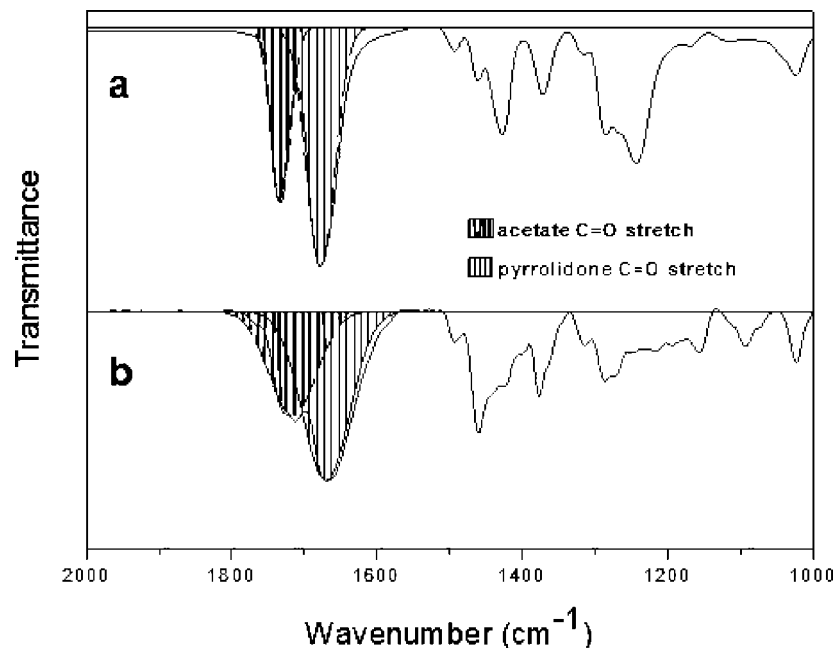


Figure 5. IR spectra of (a) pure PVP-PVAc polymer and (b) acetate-functionalized gold nanocrystals. The area ratios of the deconvoluted peaks for VP and VAc units of the samples are 1.98 and 1.92, respectively.

sensing applications based on surface plasmon resonance and surface-enhanced Raman spectroscopy.^{2,3}

Esterification of Hydroxyl-Functionalized Gold Nanocrystals. The hydroxyl group of copolymer-capped gold nanocrystals can behave as a linker to connect with various functionalities through esterification (Figure 4a). Acyl chlorides were chosen as a reactive counterpart to the hydroxyl group. Triethylamine was added to the copolymer-capped gold nanocrystals in *N,N*-dimethylacetamide (DMAc) for supplying enough basicity to remove hydrogen chloride generated during the reaction. Acetyl chloride, lauroyl chloride, and pentadecafluorooctanoyl chloride were added dropwise to the reaction mixture, followed by stirring at room temperature for 24 h. The particles were obtained after several precipitation–dispersion cycles. The carbonyl stretch of the unfunctionalized gold nanocrystals shows a sharp peak at 1682 cm^{-1} (Figure 4b). The reaction with acetyl chloride generates acetate groups on the copolymer, which induce an environment similar to that of the original PVP-PVAc on the gold surface (Figure 4c). The IR spectrum of the acetate-functionalized gold nanocrystals was compared to that of the free PVP-PVAc (Figure 5). The C=O peak maxima of the acetate (1720 cm^{-1}) and pyrrolidone amide (1670 cm^{-1}) groups are almost identical in both spectra, although the peaks of the functionalized gold nanocrystals are rather broad because of the unhomogeneous nature of the surface-anchored ligands. The area ratio of the deconvoluted C=O stretching peaks for the pyrrolidone and acetate units is 2:1 in the IR spectrum of the free PVP-PVAc polymer (Figure 5a). The corresponding two peaks of the acetate-functionalized gold nanocrystals were deconvoluted in the same way (Figure 5b), and their area ratio of pyrrolidone and acetate units was also estimated to be 2:1.²⁰ This coincidence

indicates that all acetate groups in the original PVP-PVAc were hydrolyzed to the hydroxyl groups of the PVP-PVA during the formation of the gold nanocrystals, and that the esterification with acetyl chloride completely regenerated all acetate groups. Such a quantitative conversion of the copolymers is advantageous to the effective functionalization of gold nanocrystals with various chemical and biological moieties. The average diameter of the hydroxyl-functionalized gold nanoparticles was measured to be 54 nm, and that of the acetate-functionalized nanoparticles was 47 nm by dynamic light scattering (DLS) analysis, meaning that the particles were still stable and well-dispersed in solution after the surface esterification. A slight decrease in the particle diameter is attributed to relatively hydrophobic nature of the acetate group compared to that of the original hydroxyl functionality.

The reaction with lauroyl chloride shows a spectrum similar to that of the acetate-functionalized gold nanocrystals (Figure 4d). The peak at 1728 cm^{-1} assigned to the ester C=O stretching mode appears as a shoulder of the pyrrolidone C=O peak. The reaction with pentadecafluorooctanoyl chloride has a smaller ester peak at 1776 cm^{-1} (Figure 4e), presumably due to the bulky alkyl chain of fluoro-substituted alkyl ligands lowering the reactivity. The change of the surface groups containing long alkyl chains discriminated particle dispersity in polar solvents. After the reactions, the particles were readily aggregated, whereas the original hydroxyl-functionalized particles formed a stable dispersion in ethanol. Although the reactions must be optimized under harsh conditions, various functionalities could be incorporated on the gold nanocrystals even at room temperature.

Conclusion

We present a direct synthesis of functionalized gold nanocrystals by using the copolymer both as a surface-regulating reagent and as a linker for additional functional-

(19) (a) Yang, W.-H.; Schatz, G. C.; Van Duyne, R. P. *J. Chem. Phys.* **1995**, *103*, 869–875. (b) Novotny, L.; Bian, R. X.; Xie, X. S. *Phys. Rev. Lett.* **1997**, *79*, 645–648.

ization. This simple one-pot process controls the particle morphology, and simultaneously generates multiple hydroxyl groups on the surface, which can readily conjugate with versatile functionalities. It is anticipated that the choice of well-designed copolymers would be a general methodology for the functionalized metal nanocrystals with precise shape control and serve as a new platform for various applications.

Acknowledgment. This work was supported by the Nano R&D program (2007-02668) and a grant from the Korea Science

and Engineering Foundation (KOSEF), funded by the Korean Government (MEST) (R11-2007-050-04002-0) (to C.I.Y., D.S. and H.S.), and the KRIBB Research Initiative program (to B.H.C. and I.S.C.).

CM8028609

-
- (20) Spiekermann, M. Quantitative analysis by IR spectroscopy. In *Infrared and Raman Spectroscopy: Methods and Applications*; Schrader, B., Ed.; VCH: Weinheim, Germany, 1995; pp 415–430.